Korean J. of Chem. Eng., 11(4), 261-270 (1994)

INSTABILITIES INDUCED BY AN ELECTROSTATIC FIELD OVER THE FILM FLOW DOWN AN INCLINED PLANE

Hyo Kim† and Dok Chan Kim*

R & D Training Center, Korea Gas Corporation, Il-dong 277-1, Ansan 425-150, Korea
*Department of Chemical Engineering, Seoul City University, Seoul 131-743, Korea
(Received 17 January 1994 • accepted 15 June 1994)

Abstract—A study of the instabilities in the interaction of an electrostatic field with a thin liquid film flowing under gravity down an inclined plane is presented. First, the long-wave stability conditions are studied by perturbing the evolution equation of film height about its steady-state solution. Three limits of flow systems are considered, i.e., static state, Reynolds number $Re=O(1)$ and $Re=O(1/\xi)$. Here $\xi(\ll 1)$ is the ratio of the characteristic length scale parallel to the flow to the primary film thickness. Next, the long-wave behavior of the thin film flow is examined with the electrostatic potential of a Gaussian function in the two limits of Reynolds number, i.e., $Re=O(1)$ and $Re=O(1/\xi)$. These results are also compared with those from a full-scale explicit calculation. Finally, wave-growth rates are calculated from the Orr-Sommerfeld equation to show the stability to wave number with and without the electric field. The effect of the electric field is to lessen the range of the wave number in which the thin film flow remains stable.

INTRODUCTION

The investigation of the thin liquid-film flow has attracted much attention for many years. Such thin layer of liquid acts an important role in many engineering processes due to its high transfer surface of heat and mass in comparison with the volume of through-flow. When a thin liquid film flows under gravity down an inclined plane, the film becomes unstable as Reynolds number increases, that is, traveling waves appear on the free surface. To determine this instability onset has been a big research topic. The study of the stability of thin liquid layers draining down an inclined plane was initiated by Yih [1] and Benjamin [2]. Their analysis identified regimes of linear stability of the film as a function of the Reynolds number and the angle of inclination. Yih [3] employed long-wave asymptotics, and thereby determined a critical Reynolds number. Benny [4] derived a long-wave nonlinear evolution equation for the local thickness of a thin, isothermal liquid layer on a plane surface. After this time a great number of extensions of the isothermal case has been made, such as those by Lin [5], Gjevik [6], Pumir et al. [7], and Alekseenko et al. [8], to name only a few. Their quasilinear investigations are for the height of the film as a function of time, which is solved either numerically or analytically.

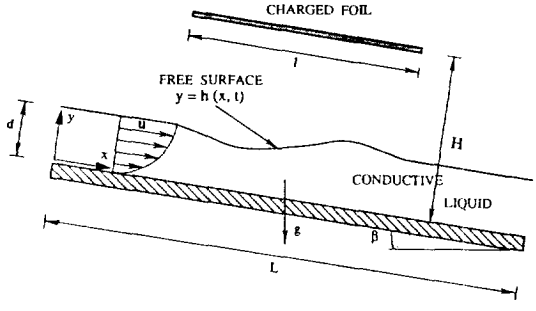

Fig. 1. The coordinate scheme of the plane flow under an electrostatic field.

The objective here is to consider the linear stabilities when an electrically conductive liquid layer flows under gravity down an inclined plane over which an electrostatic field is turned on through a chargeable foil (see Fig. 1). This kind of flow system has the following research background. The study on the interaction of an electrostatic field with a thin liquid film was started by Kim et al. [9] for a new design of lightweight space radiator to replace present-day heavy space radiator which employs armored heat pi-

†To whom all correspondences should be addressed.

pes built in by the wick materials such as nickle, copper and titanium, etc. The proposed new concept consists of an enclosed metallic-foil/ceramic-cloth, thin-film, pumped-loop radiator, in which leaks of the liquid-metal coolant caused by punctures from most micrometeorites and space debris are prevented by detecting the leak and then switching on an internal electrostatic field, that is, the applied electrostatic field makes the pressure at the puncture sufficiently below the pressure outside the radiator minus the capillary pressure and stops the leakage. In order to understand this basic effect of the electrostatic field on the film flow and to establish the feasible working ranges of the radiator, Kim et al. [10, 11] investigated two kinds of flow systems of a thin liquid layer with evolution equations for film thickness derived from the equations of motion with proper approximations. In the first, the liquid film in the presence of a gravitational body force flows along an inclined flat plate with a specified initial film height. In the zero-gravity second case, the liquid flows down the interior surface of a rotating conical pipe, where the entrance film thickness is specified at a constant angular velocity and the centrifugal force replaces the gravitational force. The pressure distribution on the solid wall was also calculated to check the possibility to prevent leakage of the coolant from a puncture. The result is that the radiator will be allowed to have thinner, or no armor, and hence there will be a considerable weight savings. Important benefits of this idea could accure to the space station, which is reported to be currently overweight and underpowered. For high-power requirements, such as propulsion systems, military applications, and large scale manufacturing and life support, this technology is considered to be critical.

In the following sections, long-wave stabilities are investigated by perturbing the evolution equation of film height about its steady-state solution in the limits of three cases of flow systems, i.e. static case, small and large Reynolds numbers. Here the static-state flow is treated as an extreme case of the film flow down an inclined plane. In addition, for the long-wave behavior of the flow systems the film height interacting with the electrostatic potential of a Gaussian function is plotted and compared with the result from a full-scale code. Wave-growth rates are also calculated to obtain stable wave numbers from the Orr-Sommerfeld equation without the thin film limits.

ELECTROHYDRODYNAMIC ANALYSIS

The flow is considered of an incompressible, viscous, thin liquid film draining down an inclined plane with gravity g. The plane is assumed to make an angle β with the horizontal, and the two-dimensional coordinate system is chosen such that the x axis is parallel to the plane and the y axis is perpendicular to it. Above the liquid film there is a vacuum, where at a distance H from the plane is a charged plate of length l, which is parallel to the x axis. The film thickness in the primary flow is defined as d and $\xi = d/L$, where L is the characteristic length scale parallel to the film (Fig. 1).

The electric field is satisfied by the Laplace's equation,

$$\nabla^2\phi = 0, \tag{1}$$

for the electric potential $\phi(x, y)$ in the fluid, ϕ', and for that in the vacuum region, ϕ''. To solve this equation the following boundary conditions are needed:

$$\phi(x, H) = FH\Phi(x), \text{ for } y = H,$$
$$\phi = 0, \text{ for } y = 0, \tag{2}$$

and along the free surface $y = h(x, t)$ the interfacial boundary conditions are

$$\phi'(x, h, t) = \phi''(x, h, t), \quad \varepsilon_f \frac{\partial \phi'}{\partial n} = \varepsilon_0 \frac{\partial \phi''}{\partial n}. \tag{3}$$

Here ε_f is the dielectric constant of the fluid, ε_0 is that of the vacuum and the partial derivative is in the direction of the outward unit normal, $\mathbf{n}$, to the interface.

The independent and dependent variables used in the governing equations of motion and the evolution equations are expressed in non-dimensional forms by letting d be the unit of length in the y direction, L the unit of length in the x direction, U_0, which will be chosen later, the unit of the x-direction velocity u, ξU_0 the unit of the y-direction velocity v, L/U_0 the unit of time t, ρU_0^2 the unit of pressure p where ρ is the fluid density, F the unit of electric field and FH the unit of electrostatic potential. Extensive calculations (Kim et al. [10]) have been performed to obtain the film thickness and the bottom pressure as functions of both space and time. Three methods of calculation were employed. For a Reynolds number of O(1), inertial effects may be neglected at leading order, and a long-wave approximation is appropriate. The Reynolds number Re is defined as

$$\mathrm{Re} = \frac{\rho U_0 d}{\mu} \tag{4}$$

where μ is the viscosity of the fluid and $U_0 = \rho g d^2 \sin(\beta)$

/3μ is the average entrance velocity. In this limit, one can derive a nonlinear evolution equation for the height h(x, t) of the film accurate to $O(\xi^2)$. This equation has been studied extensively by Kim et al. [10] and the result is

$$\frac{\partial h}{\partial t}+3h^2\frac{\partial h}{\partial x}+\xi\frac{\partial}{\partial x}\left(\frac{6}{5}Reh^6\frac{\partial h}{\partial x}-\cot(\beta)h^3\frac{\partial h}{\partial x}+\frac{2}{3}\frac{\xi^2}{Ca}h^3\frac{\partial^3 h}{\partial x^3}\right)+\frac{2}{3}\xi K\left(1-\frac{1}{\varepsilon_f}\right)\frac{\partial}{\partial x}\left(h^3\frac{\partial}{\partial x}[E^t_{0n}]^2\right)=0, \tag{5}$$

where E^x_{0n} is the normal component of the leading-order electrostatic field at the surface of the film $y=h(x, t)$, the capillary number is defined by $Ca=2\mu U_0/\sigma$ where σ is the surface tension and K, assumed to be order one, is a dimensionless electrostatic field constant:

$$K=\frac{\varepsilon_0 dF^2}{16\pi\mu U_0}. \tag{6}$$

In Eq. (5) the coefficient ξ^2/Ca is assumed to be order unity. The placement of the charged foil has to be considered to get the E_{0n}. The electric potential along $y=H$ depends on the slow x scale and the characteristic length scale in the y direction in the vacuum region is d. Hence, the leading-order electric field can be transformed from the electrostatic potential at leading order in ξ, i.e., $E^x_{0n}=H(\partial\phi^t_0/\partial y)$, where ϕ^t_0 is calculated from the Eq. (1) with the boundary conditions (2) and (3):

$$\phi^t_0=\Phi(x)\left\{1+(y-H)\left[h(x, t)\left(\frac{1}{\varepsilon_f}-1\right)+H\right]^{-1}\right\},$$
$$\text{for } h(x, t)<y<H. \tag{7}$$

For the applications a larger Reynolds number may be necessary. For this large Reynolds number, i.e., $Re=O(1/\xi)$, the inertial terms appear at lowest order, and it is necessary to use the Karman-Pohlhausen approximation to obtain an evolution equation. This has successfully been applied to other thin film problems (Thomas et al. [12] and Rahman et al. [13]). The local x-component velocity is approximated by

$$u=\frac{3q}{h}\left\{\frac{y}{h}-\frac{1}{2}\left(\frac{y}{h}\right)^2\right\}, \tag{8}$$

where q is the local flow rate defined by

$$q=\int_0^h u\,dy. \tag{9}$$

One then obtains a coupled set of nonlinear hyperbolic equations accurate to $O(\xi)$ for the height h and flow rate q. These evolution equations have been derived by Kim et al. [10] and the results are

$$\frac{\partial h}{\partial t}=-\frac{\partial q}{\partial x} \tag{10}$$

and

$$\frac{\partial q}{\partial t}+\frac{6}{5}\frac{\partial}{\partial x}\left(\frac{q^2}{h}\right)=\frac{2h}{R}\bar{K}\left(1-\frac{1}{\varepsilon_f}\right)\frac{\partial}{\partial x}(E^x_{0n})^2-\frac{3}{R}\frac{q}{h^2}+\frac{\cos(\beta)}{Fr^2}\left(\frac{h}{B}-h\frac{\partial h}{\partial x}\right), \tag{11}$$

where $\bar{K}=\xi K=O(1)$, $R=\xi Re=O(1)$, $B=\xi\cot(\beta)=O(1)$ and the Froude number is given by

$$Fr=\frac{U_0}{\sqrt{gd}}. \tag{12}$$

The previous two methods have shown asymptotic solutions of the electrohydrodynamic problem. This approach was taken because the system represents a complicated nonlinear moving boundary problem whose solution involves solving the Navier-Stokes equations coupled to the electrostatic equations. A complete numerical solution of this problem is still very difficult. Suppose that the charged foil is far away from the plane of the flowing film, this idea decouples the electrostatic problem from the fluids problem. Hence, a direct solution of the Navier-Stokes equations, using the finite-difference code SOLA [14] based on the marker-and-cell method, can be obtained in the presence of the electric field.

In the early study [10], for the electrohydrodynamic calculations the dimensionless electrostatic potential along the charged foil *l*, i.e., the value of $\Phi(x)$ was used as 1, that is, this was a specific value used for solving the Laplace's Eq. (1) of the electric potential and the solution was found in Morse and Feshbach [15]. However, in order to simulate a slowly varying potential which will make a long-wave disturbance on the thin-film flow a potential with a Gaussian function, $\Phi(x)=e^{-\alpha(x-x_0)^2}$ where a is an arbitrary constant and x_0 is the center of the electric foil, will be used later on this work to show the film-thickness variations to both space and time.

LINEAR STABILITY

The linear stability for the liquid film flow down an inclined plane was studied by Benjamin [2] and Yih [3]. In a long-wave limit their analysis identified regimes of linear stability of the film as a function of the Reynolds number and the angle of inclination:

$$\mathrm{Re}<\frac{5}{6}\cot(\beta). \tag{13}$$

The aim here is to generalize this result to include the effect of the electrostatic field on the film flow. For this purpose, three cases of flow systems are considered : static case ($\beta=0$), $\mathrm{Re}=O(1)$ and $\mathrm{Re}=O(1/\xi)$. In addition, without the thin-film limit the Orr-Sommerfeld equation is solved by the long-wave approximation. Recently the effect of a magnetic field on fluid flow down an inclined plane has been studied by Shen et al. [16].

1. Static Case : $\beta=0$

In the static case with $\beta=0$, there is no driving force for the liquid film to flow along a flat plate. When an electrostatic field is turned on through a chargeable foil, the stationary fluid will start to move toward the center of the foil and have a symmetric shape like a convex meniscus below the foil. In this case the fluid filling up the peak comes from both ends of the plate. There exists a similar approach used to the lubrication theory for the Eq. (5) except that there is none of the inertial effect and the primary flow due to gravity. The evolution equation is

$$\frac{\partial h}{\partial t}+\xi\frac{\partial}{\partial x}\left\{\left(-\frac{1}{3}\frac{\mathrm{Re}}{\mathrm{Fr}^2}\frac{\partial h}{\partial x}+\frac{2}{3}\frac{\xi^2}{\mathrm{Ca}}\frac{\partial^3 h}{\partial x^3}+\frac{2}{3}K\left[1-\frac{1}{\varepsilon_f}\right]\frac{\partial}{\partial x}[E_{0n}^{r}]^2\right)h^3\right\}=0. \tag{14}$$

To find a stability condition of this static problem the Eq. (14) needs to be perturbed about its steady-state solution h_s. Letting $h(x, t)=h_s(x)+\tilde{h}(x, t)$, where $\tilde{h}(x, t)$ represents the small-height disturbance, the film thickness at steady state is reduced to

$$h_s=1+2\frac{\mathrm{Fr}^2}{\mathrm{Re}}\frac{\xi^2}{\mathrm{Ca}}\frac{d^2h_s}{dx^2}+2\frac{\mathrm{Fr}^2}{\mathrm{Re}}K\left(1-\frac{1}{\varepsilon_f}\right)(E_{0n}^{r})^2, \tag{15}$$

where the boundary conditions that $h_s\to 1$ and $E_{0n}^{r}\to 0$ as $x\to\pm\infty$ (with $x_0=0$ as the center of the foil) are used. And the linearized disturbance equation for $\tilde{h}(x, t)$ becomes

$$\frac{\partial\tilde{h}}{\partial t}=\frac{1}{3}\xi\frac{\partial}{\partial x}\left\{h_s^3\left(\frac{\mathrm{Re}}{\mathrm{Fr}^2}\frac{\partial\tilde{h}}{\partial x}-2\frac{\xi^2}{\mathrm{Ca}}\frac{\partial^3\tilde{h}}{\partial x^3}\right)\right\}. \tag{16}$$

With setting $\tilde{h}(x, t)=e^{ct}\Theta(x)$ and substituting into the Eq. (16), the eigenvalue c is determined to get a linear stability condition of this problem for all ranges of the parameters. The result after proper manipulations is given by

$$c=-\xi\frac{\int_{-\infty}^{\infty}h_s^3\left(\frac{\mathrm{Re}}{\mathrm{Fr}^2}\Theta_x^2+\frac{3\xi^2}{\mathrm{Ca}}\Theta_{xx}^2+\frac{2\mathrm{Fr}^2}{\mathrm{Re}}\frac{\xi^4}{\mathrm{Ca}^2}\Theta_{xxx}^2\right)dx}{3\int_{-\infty}^{\infty}\left(\Theta^2+\frac{\mathrm{Fr}^2}{\mathrm{Re}}\frac{\xi^2}{\mathrm{Ca}}\Theta_x^2\right)dx}, \tag{17}$$

where the subscript x denotes the derivative with respect to x. As we can see, the value c is negative for all the parameters. Hence this static problem is always linearly stable. The Eq. (17) has only stabilizing effects of gravity and surface tension.

2. Order One Reynolds Number : $\mathrm{Re}=O(1)$

Considering a linear stability analysis in the limitation of lubrication theory, the Eq. (5) is perturbed about its steady-state solution, i.e., by setting $h(x, t)=1+\tilde{h}(x, t)$, where the small disturbance $\tilde{h}$ is assumed a sinusoidal function $\tilde{h}=e^{i\alpha(x-ct)}$. Here $\alpha\geq 0$ is the wave number of the disturbance and c is the complex wave speed. The electric field E_{0n}^{r} is obtained from the Eq. (7), i.e., $E_{0n}^{r}=H\Phi(x)/\{H+h(1/\varepsilon_f-1)\}$. The effect of variations of h on the electric field is accounted. And for the similar disturbance in ϕ^r as in the liquid film, the length of the foil is assumed to have the same dimension as that of the inclined plane, i.e., $l\to\infty$. Supposing that $\Phi(x)=1$, the evolution Eq. (5) is linearly stable when

$$\mathrm{Re}<\frac{5}{6}\cot(\beta)\sim\frac{10}{9}K\frac{H^2(1-1/\varepsilon_f)^2}{(1/\varepsilon_f+H-1)^3}+\frac{5}{9}\frac{\xi^2}{\mathrm{Ca}}\alpha^2. \tag{18}$$

Here we can see that the electric field is a destabilizing effect but the surface tension makes the film stable. If there are no electric field and surface tension in the above equation, the result has the same stability condition derived by Benjamin and Yih.

3. Large Reynolds Number : $\mathrm{Re}=O(1/\xi)$

As with the order unity Reynolds number case, a linear stability analysis for this $\mathrm{Re}=O(1/\xi)$ case can be done. The definitions of the dimensionless constants show that

$$\frac{\mathrm{Re}\sin(\beta)}{3\mathrm{Fr}^2}=1. \tag{19}$$

Therefore a steady-state solution of the Eqs. (10) and (11) exists of the form $h=1$ and $q=1$. Letting η represent the perturbation of h from the uniform height, i.e., $h=1+\eta$, the linearized disturbance equation can be derived from the nonlinear hyperbolic Eqs. (10) and (11):

$$\frac{\partial^2\eta}{\partial t^2}+\frac{12}{5}\frac{\partial^2\eta}{\partial t\partial x}+\left(\frac{6}{5}-\frac{3B}{R}+\frac{6\bar{K}(1-1/\varepsilon_f)^2H^2}{R[1/\varepsilon_f+H-1]^3}\right)\frac{\partial^2\eta}{\partial x^2}+\frac{3}{R}\frac{\partial\eta}{\partial t}+\frac{9}{R}\frac{\partial\eta}{\partial x}=0. \tag{20}$$

Looking for a time harmonic solution proportional to $e^{i\alpha(x-ct)}$, where α is the real wave number and $c=c_r+ic_i$ is the complex frequency, the dispersion relation from the Eq. (20) is given by

$$c^2-\frac{12}{5}c+\left(\frac{6}{5}-\frac{3B}{R}+\frac{6\bar{K}(1-1/\varepsilon_f)^2H^2}{R[1/\varepsilon_f+H-1]^3}\right)+\frac{3i}{\alpha R}(c-3)=0. \quad (21)$$

The condition for onset can be determined from the Eq. (21) by requiring that the first and the second derivatives of c_i with respect to α vanish exactly. The result of this calculation is that the critical Reynolds number, Re_c, and the wave number, α_c are given by

$$Re_c=\cot(\beta)-2K\frac{H^2(1-1/\varepsilon_f)^2}{[1/\varepsilon_f+H-1]^3},\quad \alpha_c=0. \quad (22)$$

The critical Reynolds predicted in this limit differs from that in the order unity Reynolds number limit. This situation comes from the different magnitude of the Reynolds number and the approximation (8) used for the velocity profile. Without the electric field this flow system is studied by Prokopiou et al. [17].

4. Orr-Sommerfeld Equation

In the absence of the thin-film limit, that is, assuming that the length scales in the vertical and horizontal directions are the same ($\xi=1$), that the length of the plate is infinite, and that $\Phi(x)=1$ as in the thin-film cases, a steady parallel flow can be found with the velocity and pressure given by

$$u_0=\frac{Re\sin(\beta)}{Fr^2}\left(y-\frac{1}{2}y^2\right),$$
$$p_0=\frac{\cos(\beta)}{Fr^2}(1-y)+\frac{2KH^2}{Re}\left(\frac{1}{\varepsilon_f}-1\right)\left(\frac{\partial\phi_0^e}{\partial y}\right)^2, \quad (23)$$

and the electric potential [10, 11, 18]

$$\phi_0^e=1+(y-H)\left(\frac{1}{\varepsilon_f}+H-1\right)^{-1},\ \text{for } 1<y<H. \quad (24)$$

Following Benjamin [2] and Yih [3], $u=u_0+\tilde{u}$, $v=\tilde{v}$, $p=p_0+\tilde{p}$, $h=1+\tilde{h}$ and $\phi^e=\phi_0^e+\tilde{\phi}^e$ are introduced into the equations of motion and then solved for the same order of magnitude, where the small-amplitude disturbances are denoted by an overtilde. For the linear stability the following time-harmonic assumptions are applied:

$$\tilde{u}=\psi'(y)e^{i\alpha(x-ct)},$$
$$\tilde{v}=-i\alpha\psi(y)e^{i\alpha(x-ct)},$$
$$\tilde{p}=f(y)e^{i\alpha(x-ct)},$$
$$\tilde{h}=g(y)e^{i\alpha(x-ct)},$$
$$\tilde{\phi}^e=q(y)e^{i\alpha(x-ct)}, \quad (25)$$

where the prime represents the derivative with y. Finally the linearized Navier-Stokes equations are reduced to the Orr-Sommerfeld equation for $\psi=\psi(y)$,

$$\psi''''(y)-2\alpha^2\psi''(y)+\alpha^4\psi(y)=i\alpha Re\{(u_0-c)[\psi''-\alpha^2\psi(y)]-u_0''\psi'\}. \quad (26)$$

The boundary conditions along $y=0$ are

$$\psi(0)=\psi'(0)=0, \quad (27)$$

while along $y=1$

$$\psi''(1)+\left(\alpha^2-\frac{3}{c-3/2}\right)\psi(1)=0 \quad (28)$$

and

$$-3\alpha\cot\beta\frac{\psi(1)}{c-3/2}+\alpha Re\left(c-\frac{3}{2}\right)\psi'(1)-i\psi'''(1)+3i\alpha^2\psi'(1)+\alpha\frac{\psi(1)}{c-3/2}\left(-\frac{2\alpha^2}{Ca}+KW\right)=0, \quad (29)$$

where the constant W is given by

$$W=\alpha H^2\left(1-\frac{1}{\varepsilon_f}\right)\left(\frac{1}{\varepsilon_f}+H-1\right)^{-2}\left\{\frac{1}{\varepsilon_f}\tanh(\alpha)+\tanh[\alpha(H-1)]\right\}^{-1}. \quad (30)$$

This is a linear eigenvalue problem for the complex eigenvalue $c=c_r+ic_i$. In the long wave limit, i.e., $\alpha\to0$, the uniform flow is stable if

$$Re<\frac{5}{6}\cot(\beta)-\frac{10}{9}KW, \quad (31)$$

where in the long wave limit,

$$W\to\frac{H^2(1-1/\varepsilon_f)^2}{[(1/\varepsilon_f)+H-1]^3}. \quad (32)$$

This is the same result as in the case of $Re=O(1)$ except for the effect of the surface tension. The eigenvalue problem (26)-(29) is solved numerically in the next section by using a shooting method [19].

NUMERICAL COMPUTATIONS

1. Deformation of Film Surface

In the previous section 2 two asymptotic evolution equations in the film thickness h are represented for the electrohydrodynamic calculations. This approach was taken because the system contains a complicated nonlinear moving boundary problem coupled to the electrostatic equation. Assuming $H\gg1$ so that the

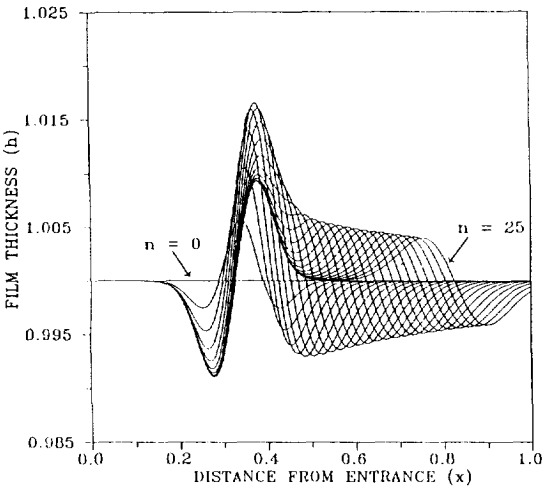

Fig. 2. Free surface profiles determined by Eq. (5) for t= 0.01 n, n=1,⋯,25 with F=0.5 kV/cm, β=0.1 rad., d=0.15 cm, g=2 cm/sec², σ=0, Re=3.78, K=0.9, H=13(1/3), and the other parameter for lithium at 700 K.

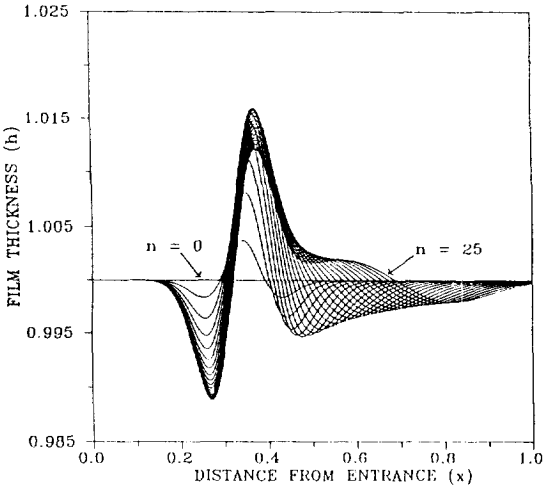

Fig. 3. Free surface profiles determined by SOLA for t= 0.01 n, n=1,⋯,25 with F=0.5 kV/cm, β=0.1 rad., d=0.15 cm, g=2 cm/sec², σ=0, Re=3.78, K=0.9, H=13(1/3), and the other parameter for lithium at 700 K.

charged foil is far away from the plane of the flowing film, the electrostatic problem is decoupled from the fluid problem. Hence, if a solution of the electrostatic problem is determined, the Navier-Stokes equations can be solved with a known forcing function of the electric field. This moving boundary problem is solved by using the full-scale code SOLA [14]. In order to simulate a slowly varying potential, $\Phi(x)$ is set by $e^{-100(x-1/3)^2}$. Here the location of the charged-foil center is taken as $x=1/3$.

The solutions of the approximate long-wavelength models (5), and (10) and (11) will now be compared with the solutions from the SOLA. Clearly, solving either (5) or (10) and (11) is a much easier and faster task than solving the Navier-Stokes equations. Hence, if the approximate models can be shown to make good predictions in the range of interest of parameters, this justifies their usefulness. U_0 is chosen as the mean velocity of a steady parallel flow down an inclined plane and proportional to d^2. Here the physical parameters are taken for lithium at 700 K ($\mu=0.0038$ poise, $\sigma=363.2$ dyne/cm, and $\rho=0.493$ g/cm^3) and the fluid is a perfect conductor, i.e., $\varepsilon_f\to\infty$. As U_0 varies, Re, Fr, Ca vary linearly with U_0, while K is inversely proportional to U_0. For fixed electric field F, K changes as the Reynolds number changes. The effect of surface tension is neglected because there is no regions of large curvature on the free surfaces with the slowly varying potential and the main concern is to show how well solutions of the approximate models compare with the solutions of the full system of equations. The solution of the lubrication model (5) begins with a fourth-order Runge-Kutta, and then continues with the Hamming's predictor-corrector method. The nonlinear hyperbolic Eqs. (10) and (11) are solved by using a two-step Lax-Wendroff method with diffusion and antidiffusion [20]. The steady flow down an inclined plane is chosen as an initial condition and the upstream boundary condition is steady Poiseuille flow. At $t=0$ the electric field is turned on and the interface is determined.

To calculate the change of the unsteady free surface when $Re=O(1)$, the following properties, i.e., $F=0.5$ kV/cm, $\beta=0.1$ rad., $d=0.15$ cm, $g=2$ cm/sec² and $\sigma=0$, are taken. This will give us $Re=3.78$, $K=0.9$, $\xi=0.0025$ and $H=13(1/3)$. In Fig. 2 the dimensionless film thickness h is plotted from the Eq. (5) as a function of x for $t_n=0.01$ n, $n=1,\cdots,25$. As t increases the initial perturbation in height grows in absolute magnitude until a steady state is approached. As we can expect from the linear stability condition (18), the perturbed wave becomes stable at this Reynolds number, i.e., $Re_c\to 8.22$ as $\alpha\to 0$. To compare this approximate model with the exact numerical prediction, the film height h from the SOLA is plotted in Fig. 3. And for a clear view the steady-state lubrication result is plotted in Fig. 4 along with the last plot of Fig. 3. The surface deformation is similar to that of the exact an-

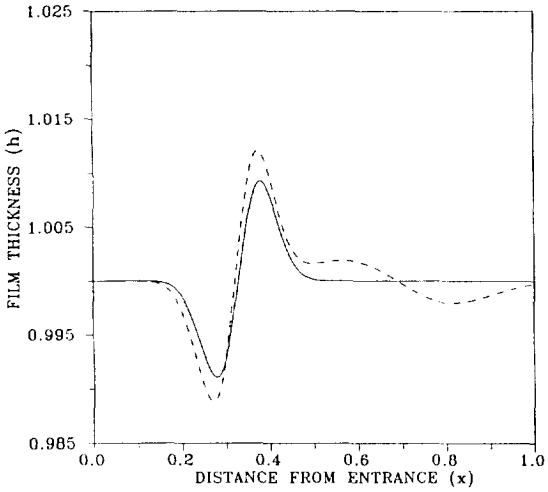

Fig. 4. Free surface profiles determined by the steady-state lubrication result (---) and the last computed time step shown in Fig. 3 (—).

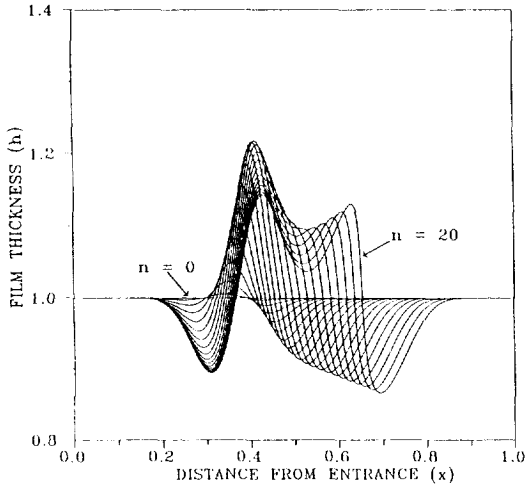

Fig. 5. Free surface profiles determined by Eqs. (10) and (11) for t=0.01 n, n=1,⋯,20 with F=20 kV/cm, β=0.1 rad., d=0.15 cm, g=100 cm/sec², σ=0, Re=189.0, K=28.87, H=13(1/3), and the other parameter for lithium at 700 K.

swer except that the absolute magnitude of the perturbation in height is a little less. This means that in the real system the inertial force is a slightly more dominating than the viscous effect at this Reynolds number.

For a large Reynolds number case: $Re=O(1/\xi)$, an increased gravity $g=100$ cm/sec² is applied and at the same time the electric field is increased to 20 kV/cm

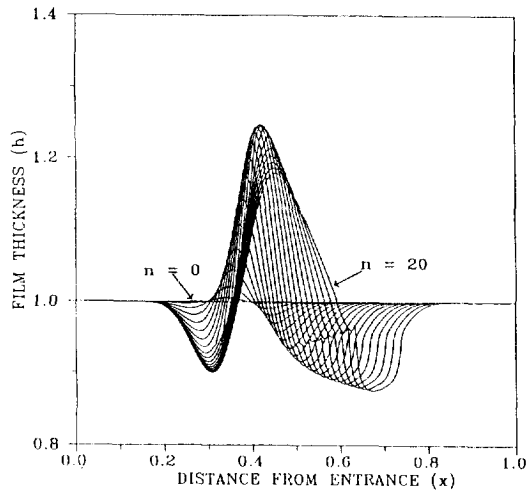

Fig. 6. Free surface profiles determined by SOLA for t=0.01 n, n=1,⋯,20 with F=20 kV/cm, β=0.1 rad., d=0.15 cm, g=100 cm/sec², σ=0, Re=189.0, K=28.87, H=13(1/3), and the other parameter for lithium at 700 K.

for the compensation of the decreased K as U_0 increases, while keeping the other parameters as in the $Re=O(1)$ case. The effect of this is to raise the Reynolds number and the dimensionless electrostatic constant, to $Re=189.0$, and $K=28.87$. For this case the time-dependent Karman-Pohlhausen model (10) and (11) is solved and plotted in Fig. 5 for $t_n=0.01$ n, n=1,⋯,20. As in the smaller Reynolds number case, the height of the film under the foil at first decreases with increasing x and then increases. The film will now rise up to about 20% of its equilibrium height. The maximum height at steady state is around h=1.15. As time increases note that a disturbance will begin along the precursor through, this will develop into a shock. We can expect this instability from the result of the linear stability condition (22) at this large Reynolds number. However this event is harmless to this system, since the shock occurs downstream of the foil and finally it will be washed away. In Fig. 6 the result from the exact numerical solution is plotted. There are qualitative similarities in the shape and speed of propagation of the disturbance. There are some quantitative differences. In particular, the shock appears to develop in a different way. The time-dependent problem is only computed up to the time of formation of the shocks. Both models will approach a steady-state solution under the foil. In Fig. 7 the steady-state film thickness from the Karman-Pohlhausen model is plotted along with the last computed re-

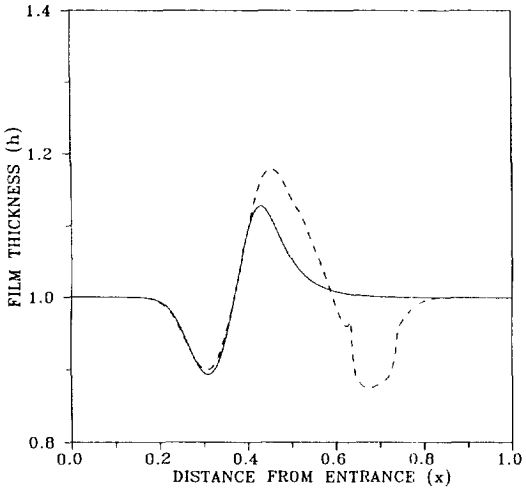

Fig. 7. Free surface profiles determined by the steady-state Karman-Pohlhausen result (---) and the last computed time step shown in Fig. 6 (—).

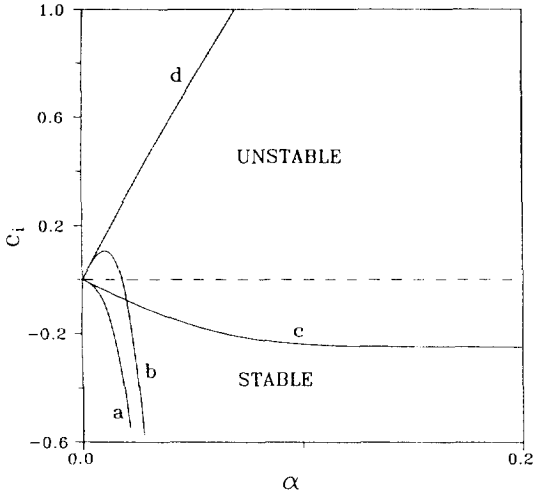

Fig. 8. α vs c_i for Re=5, β=0.1 rad., and H=13(1/3). (a) K=0 and Ca=1.35×10^{-5}. (b) K=2.73×10^{4} and Ca=1.35×10^{-5}. (c) K=0 and Ca=∞. (d) K=2.73×10^{4} and Ca=∞.

sult shown in Fig. 6. Note that the disturbance under the foil is very close to the exact profile. The approximation model has a good prediction of the real interface deformation.

2. Wave-growth Rates

In the previous section the linear stability of the liquid film flow with the effect of the electrostatic field is examined in the long wave limit. In order to understand the effect of the electric field on the stability for larger wave numbers, the eigenvalue problem (26)-(29) needs to be solved numerically. The Orr-Sommerfeld Eq. (26) is a 4th-order complex ordinary differential equation with the complex two-point boundary values (27)-(29) and this can be solved by using a shooting method. Here for one method to observe the stability regime the wave-growth rates are computed for Re=5 and Re=20. These two Reynolds numbers are selected for example calculations since the critical Reynolds number resulted from the long wave limit, i.e., from the Eq. (31), is 8.3 [=5/6 cot (0.1 rad.)] in the absence of electric field, that is, the flow will be stable at Re=5 and unstable at Re=20 as $\alpha\to0$. At Re=5 the wave number α versus the imaginary wave speed c_i is plotted in Fig. 8 for the cases of F=0 and F=100 kV/cm (K=2.73×10^{4}) combined without and with surface tension effect (Ca=1.35×10^{-5}). For positive α, if c_i is negative, the flow is linearly stable, while if c_i is positive, the flow is linearly unstable. Note that with surface tension in both K=0 and K=2.73×10^{4} the flow is much more stable than the case without surface tension. The most unstable case is the flow with electric field and at the same time without surface tension as we can expect from the thin-film limit model. With electric field and surface tension the most unstable wave number is about 0.015 (see b in Fig. 8). In Fig. 9 the growth rates are depicted at Re=20. Here the increased Reynolds number makes K de-

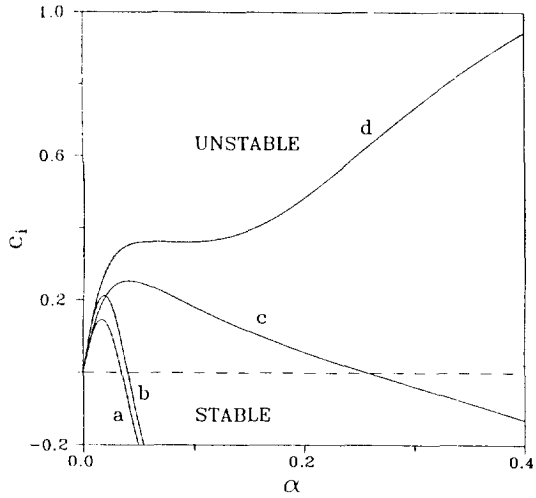

Fig. 9. α vs c_i for Re=20, β=0.1 rad., and H=13(1/3). (a) K=0 and Ca=5.4×10^{-5}. (b) K=6.82×10^{3} and Ca=5.4×10^{-5}. (c) K=0 and Ca=∞. (d) K=6.82×10^{3} and Ca=∞.

crease and Ca increase, i.e., $K=6.82\times10^{3}$ and $Ca=5.4\times10^{-5}$. Without the K effect, that in the long wave limit the flow at this Reynolds number is unstable is expected from the analysis in the section 3. The qualitative phenomena of growth rates in the four cases of flow are similar to those in Fig. 8 except that all flows are unstable as $\alpha\to0$. As Reynolds number increases the most unstable wave number is getting bigger, that is, the system becomes unstable even in a smaller wave length.

CONCLUSIONS

The purpose of this investigation is to study the instabilities in the interaction of an electrostatic field with a thin liquid film flowing down an inclined plane, and to examine the long-wave modes of the film flow with the electric potential of a Gaussian function. The electrostatic field over the film flow has perturbed the interface under the charged foil due to the effect on the change of the normal stress condition and then induced a traveling wave to be considered for its stability.

The linear stability conditions are derived for the approximation models of $Re=O(1)$ and $Re=O(1/\xi)$. The result of lubrication model coincides with the result from the Orr-Sommerfeld equation in the long-wave limit, while the Karman-Pohlhausen approximation has a different form due to the large magnitude of the Reynolds number and the assumed parabolic velocity profile. In the static-state case considered for reference the flow is always stable since there is only stabilizing effects of gravity and surface tension on the perturbed liquid film. The linear stability analysis indicates that the presence of the electric field reduces the value of the critical Reynolds number at which the flow becomes unstable.

The evolution equations for the thin-film approximate models allow easy predictions of the deformation of the interface with the electric potential of a Gaussian function. In the case of small Reynolds number $Re=3.78$, the film flow becomes stable as the perturbed wave is traveling in the down stream. However at $Re=189.0$ the wave develops into a shock and the liquid filmis unstable. To confirm the effect of the electric field on the stability when wave number increases, the Orr-Sommerfeld equation is solved numerically to show the wave-growth rates. Four kinds of flow systems are considered, i.e., a) $K=0$, $Ca\neq\infty$, b) $K\neq0$, $Ca\neq\infty$, c) $K=0$, $Ca=\infty$ and d) $K\neq0$, $Ca=\infty$. The most unstable case is d), i.e., the flow with the electric field and without the surface tension. As Reynolds number increases, the range of unstable wave numbers is increased for all the four cases.

ACKNOWLEDGEMENT

H. Kim is very grateful to Prof. S. G. Bankoff in Chemical Engineering Dept. and Prof. M. J. Miksis in Engineering Sciences and Applied Mathematics Dept., Northwestern University, for their good advice and discussion for this work, and also thanks C. W. Hirt, Flow Sciences, Inc., for the use of SOLA.

REFERENCES

1. Yih, C.-S.: *Quart. Appl. Math.*, **13**, 434 (1955).
2. Benjamin, T. B.: *J. Fluid Mech.*, **2**, 554 (1957).
3. Yih, C.-S.: *Phys. Fluids*, **5**, 321 (1963).
4. Benney, D. J.: *J. Math. Phys.*, **45**, 150 (1966).
5. Lin, S.-P.: *J. Fluid Mech.*, **63**, 417 (1974).
6. Gjevik, B.: *Phys. Fluids*, **13**, 1918 (1970).
7. Pumir, A., Manneville, P. and Pomeau, Y.: *J. Fluid Mech.*, **135**, 27 (1983).
8. Alekseenko, S. V., Nakoryakov, V. E. and Pokusaev, B. G.: *Int. J. Multiphase Flow*, **11**, 607 (1985).
9. Kim, H., Miksis, M. J. and Bankoff, S. G.: Proc. Eighth Symp. on Space Nuclear Power Systems, Albuquerque, NM, CONF-910116, 1280 (1991).
10. Kim, H., Bankoff, S. G. and Miksis, M. J.: *Phys. Fluids. A*, **4**, 2117 (1992).
11. Kim, H., Bankoff, S. G. and Miksis, M. J.: *AIAA J. Propulsion and Power*, **9**, 245 (1993).
12. Thomas, S., Hankey, W. L., Faghri, A. and Swanson, T. D.: Proc. Natl. Heat Transfer Conf., **110**, 103 (1989).
13. Rahman, M. M., Faghri, A., Hankey, W. L. and Swanson, T. D.: Proc. Natl. Heat Transfer Conf., **110**, 161 (1989).
14. Hirt, C. W., Nichols, B. D. and Romero, N. C.: "SOLA-A Numerical Solution Algorithm for Transient Fluid Flow", Los Alamos Scientific Lab., Los Alamos, NM (1975).
15. Morse, P. M. and Feshbach, H.: "Methods of Theoretical Physics", McGraw-Hill, NY (1953).
16. Shen, M. C., Sun, S. M. and Meyer, R. E.: *Phys. Fluids A*, **3**, 439 (1991).
17. Prokopiou, T., Cheng, M. and Chang, H.-C.: *J. Fluid Mech.*, **222**, 665 (1991).
18. Kim, H. and Yoo, M. H.: *Korean J. of Chem. Eng.*, **10**, 106 (1993).
19. Press, W. H., Flannery, B. P., Teukolsky, S. A. and

Vetterling, W. T.: "Numerical Recipes", Cambridge U. P., Cambridge (1986).
20. Sod, G. A.: "Numerical Methods in Fluid Dynamics: Initial and Initial Boundary-Value Problems", Cambridge U. P., NY (1985).